The impact of different external sources of iron on the global carbon cycle

Alessandro Tagliabue, Olivier Aumont, Laurent Bopp

▶ **To cite this version:**

Alessandro Tagliabue, Olivier Aumont, Laurent Bopp. The impact of different external sources of iron on the global carbon cycle. Geophysical Research Letters, 2014, 41 (3), pp.920-926. 10.1002/2013GL059059 . hal-01128894

HAL Id: hal-01128894
https://hal.science/hal-01128894

Submitted on 6 May 2021

HAL is a multi-disciplinary open access archive for the deposit and dissemination of scientific research documents, whether they are published or not. The documents may come from teaching and research institutions in France or abroad, or from public or private research centers.

L'archive ouverte pluridisciplinaire **HAL**, est destinée au dépôt et à la diffusion de documents scientifiques de niveau recherche, publiés ou non, émanant des établissements d'enseignement et de recherche français ou étrangers, des laboratoires publics ou privés.

AGU PUBLICATIONS

Geophysical Research Letters

RESEARCH LETTER
10.1002/2013GL059059

Key Points:
- Atmospheric CO_2 is relatively insensitive to changes to dust supply of iron
- Hydrothermal Fe is key to the iron inventory, but has a small effect on CO_2
- There are unexpected changes to Si cycling due to changes in Fe input

Supporting Information:
- Readme
- Text S1
- Figure S1
- Figure S2
- Figure S3

Correspondence to:
A. Tagliabue,
a.tagliabue@liverpool.ac.uk

Citation:
Tagliabue, A., O. Aumont, and L. Bopp (2014), The impact of different external sources of iron on the global carbon cycle, *Geophys. Res. Lett.*, *41*, 920–926, doi:10.1002/2013GL059059.

Received 23 DEC 2013
Accepted 14 JAN 2014
Accepted article online 17 JAN 2014
Published online 5 FEB 2014

The impact of different external sources of iron on the global carbon cycle

Alessandro Tagliabue[1], Olivier Aumont[2], and Laurent Bopp[3]

[1]Department of Earth, Ocean and Ecological Sciences, School of Environmental Sciences, University of Liverpool, Liverpool, UK, [2]Laboratoire de Physique des Océans, Centre IRD de Bretagne, Plouzané, France, [3]Laboratoire des Sciences du Climat et l'Environnment, CNRS-CEA-UVSQ, Gif sur Yvette, France

Abstract Variable supply of iron to the ocean is often invoked to explain part of past changes in atmospheric CO_2 (CO_{2atm}). Using model simulations, we find that CO_{2atm} is sensitive on the order of 15, 2, and 1 ppm to sedimentary, dust, and hydrothermal iron input. CO_{2atm} is insensitive to dust because it is not the major iron input to the Southern Ocean. Modifications to the relative export of $Si(OH)_4$ to low latitudes are opposite to those predicted previously. Although hydrothermalism is the major control on the iron inventory in ~25% of the ocean, it remains restricted to the deep ocean, with minor effects on CO_{2atm}. Nevertheless, uncertainties regarding the iron-binding ligand pool can have significant impacts on CO_{2atm}. Ongoing expansion of iron observations as part of GEOTRACES will be invaluable in refining these results.

1. Introduction

The role of the micronutrient iron (Fe) in governing phytoplankton primary productivity and the carbon cycle has become well established [e.g., *Boyd and Ellwood*, 2010]. By limiting phytoplankton growth in regions important for air-sea CO_2 transfer, Fe-mediated changes to export production have the potential to drive significant changes in atmospheric CO_2 levels (CO_{2atm}). Contemporary Fe limitation has resulted in unused, macronutrient (NO_3 and PO_4) stocks in the equatorial Pacific, subarctic Pacific, the north Atlantic, and, largest of all, in the Southern Ocean. Crucial in the Fe cycle is the process of organic complexation [*Gledhill and Buck*, 2012], which retains Fe in the dissolved pool (DFe).

Early studies suggested CO_{2atm} reductions of >70 ppm if macronutrients in the Southern Ocean were fully depleted [*Sarmiento and Orr*, 1991], seemingly supportive of variations in dust supply of Fe-driving glacial-interglacial CO_{2atm} fluctuations [*Martin*, 1990]. However, complete macronutrient depletion is rarely possible when the direct effect of Fe is modeled due to other limiting factors (e.g., light and/or macronutrients) [*Aumont and Bopp*, 2006]. A recent review [*Kohfeld and Ridgwell*, 2009] reports changes in CO_{2atm} between 5 and 20 ppm, with a central estimate of 15 ppm in response to dust Fe fertilization. Changing Fe supply has also been proposed to impact CO_{2atm} indirectly via the "silicic acid leakage" hypothesis [*Matsumoto et al.*, 2002] that suggests greater dust Fe supply during glacial periods would alleviate Fe limitation and reduce the silicification of diatoms. Greater $Si(OH)_4$, relative to NO_3, should then be transported to low latitudes, allowing diatoms to outcompete resident calcifying plankton therein and the increase alkalinity lowers CO_{2atm} [*Matsumoto et al.*, 2002; *Kohfeld and Ridgwell*, 2009]. Whether by directly or indirectly, variations in dust Fe supply are frequently invoked as a driver of CO_{2atm} variability [e.g., *Lourantou et al.*, 2010; *Martinez-Garcia et al.*, 2011; *Ziegler et al.*, 2013].

Recently, sedimentary [e.g., *Moore and Braucher*, 2008; *Tagliabue et al.*, 2009] and hydrothermal [*Tagliabue et al.*, 2010] Fe sources have also been highlighted, and there are differences in the degree of Southern Ocean dust deposition [*Huneeus et al.*, 2011]. Outstanding questions also remain regarding the role of iron-binding ligands in buffering the DFe pool [*Gledhill and Buck*, 2012] thereby modulating the biological impact. In this study, we use a state of the art ocean general circulation and biogeochemistry model with a number of different Fe sources and representations of Fe cycling to assess the impact on CO_{2atm} during long time scale simulations.

2. Methods

2.1. Biogeochemical Model

We use the latest version of the NEMO-PISCES model (v3.5, www.nemo-ocean.eu). Briefly, the biogeochemical component PISCES includes two phytoplankton functional types, two zooplankton, two particle size classes, five

©2014. American Geophysical Union. All Rights Reserved.

Table 1. A Summary of the Model Experiments Conducted, the Dust Model Used, and the Change in Atmospheric CO_2, Carbon Export, Input of Iron, and Average Preformed PO_4 That Results[a]

Simulation	Dust Source	ΔCO_{2atm} (ppm)	ΔC_{EX} (Pg C yr^{-1})	ΔFe_{IN} (Gmol Fe)	PO_{4PRE} (mmol L^{-1})
CTL_{INCA}	INCA	0 (280)	0 (7.10)	0 (72.8)	1.733
$NODUST_{INCA}$	INCA	+1.8	−0.06	−32.7	1.741
$NOSED_{INCA}$	INCA	+14.5	−0.52	−26.6	1.770
$NOHYD_{INCA}$	INCA	+1.1	−0.02	−13.5	1.737
CTL_{NCAR}	NCAR	0 (280)	0 (7.14)	0 (77.6)	1.731
$NODUST_{NCAR}$	NCAR	+2.3	−0.11	−37.5	1.741
$NOSED_{NCAR}$	NCAR	+13.5	−0.44	−26.6	1.765
$NOHYD_{NCAR}$	NCAR	+1.0	−0.01	−13.5	1.735
$NOSEDHYD_{INCA}$	INCA	+14.5	−0.52	−40.1	1.770
$DLIG_{INCA}$	INCA	−5.4	+0.15	0	1.716
$HLIG_{INCA}$	INCA	+5.1	−0.14	0	1.749
$NOSED_{HLIG\text{-}INCA}$	INCA	+18.2	−0.63	−26.6	1.780
$NOSED_{DLIG\text{-}INCA}$	INCA	+10.0	−0.37	−26.6	1.758

[a]DLIG and HLIG refer to doubled and halved ligand concentrations, respectively. CTL refers to Control Simulation.

limiting nutrients (NO_3, PO_4, DFe, NH_4, and $Si(OH)_4$), oxygen, dissolved inorganic carbon, dissolved organic carbon, alkalinity, calcite, and biogenic silica. The full carbon system is simulated [*Aumont and Bopp*, 2006], which permits the calculation of the ocean partial pressure of CO_2 (pCO_2) and associated air-sea fluxes. Fe is explicitly simulated in the dissolved pool, two particle fractions, and the biological compartments (since Fe uptake is considered independently). DFe is removed by scavenging, with free Fe explicitly calculated using a fixed ligand concentration (0.6 nM) and conditional stability (10^{12} M^{-1}), alongside additional colloidal pumping DFe losses. Scavenging rates depend on particle concentrations and scavenged Fe is returned to DFe via dissolution. Modeled DFe fields are compared to a recent observational compilation [*Tagliabue et al.*, 2012] and other biogeochemical tracers are evaluated in the supporting information.

Concerning sources, PISCES accounts for the external DFe supply from dust, continental margin sediments, hydrothermal vents, and rivers, with sea ice incorporation/release of dissolved Fe similar to *Lancelot et al.* [2009]. Dust supply is either from the INCA [*Huneeus et al.*, 2011] or National Center for Atmospheric Research (NCAR) [*Mahowald et al.*, 2005] models assuming constant solubility of 2%. Sedimentary input varies as a function of sediment oxygenation, itself a function of shelf depth [*Middelburg et al.*, 1997] using high-resolution bathymetry [*Aumont and Bopp*, 2006]. Hydrothermal input is driven by ridge spreading rate [*Tagliabue et al.*, 2010], increased to account for new observations [*Saito et al.*, 2013]. The total DFe flux is 26.9 and 13.5 Gmol DFe from sediments and hydrothermalism, respectively, with a dust providing 32.7 or 37.5 Gmol DFe from the INCA or NCAR models, respectively. While the NCAR model only has slightly more total dust supply, it has a factor of 3.8 more south of 30°S, making these two dust models good candidates for exploring the CO_{2atm} sensitivity to differing levels of Southern Ocean dust input [*Wagener et al.*, 2008].

2.2. Experimental Design

We spun up the model for 1000 years with dust from INCA (PISCES-INCA) and NCAR (PISCES-NCAR) and coupled to a well-mixed CO_{2atm} reservoir (initialized with a preindustrial value of 280 ppm) that is adjusted due to simulated air-sea fluxes. After the spin up, the air-sea CO_2 flux drift was $<4 \times 10^{-5}$ Pg C or <0.25% and total annual ocean productivity, export production and air-sea CO_2 exchange were similar at ~39, 7.1, and −0.013 Pg C, respectively, for PISCES-INCA and PISCES-NCAR. We then launched six separate simulations where dust, sediment, and hydrothermal Fe sources were each removed (plus a control) for both PISCES-INCA and PISCES-NCAR (see Table 1). To this initial set of simulations we conducted a further five where sediment and hydrothermal sources were both removed, ligand concentrations were halved or doubled, and sediment sources were eliminated in combination with halved or doubled ligand concentrations. To determine the net impact of these perturbations on CO_{2atm} and ocean biogeochemistry, rather than the initial adjustment, all experiments were 300 years (by which time the drift in anomalous air-sea fluxes was negligible, supporting information).

©2014. American Geophysical Union. All Rights Reserved.

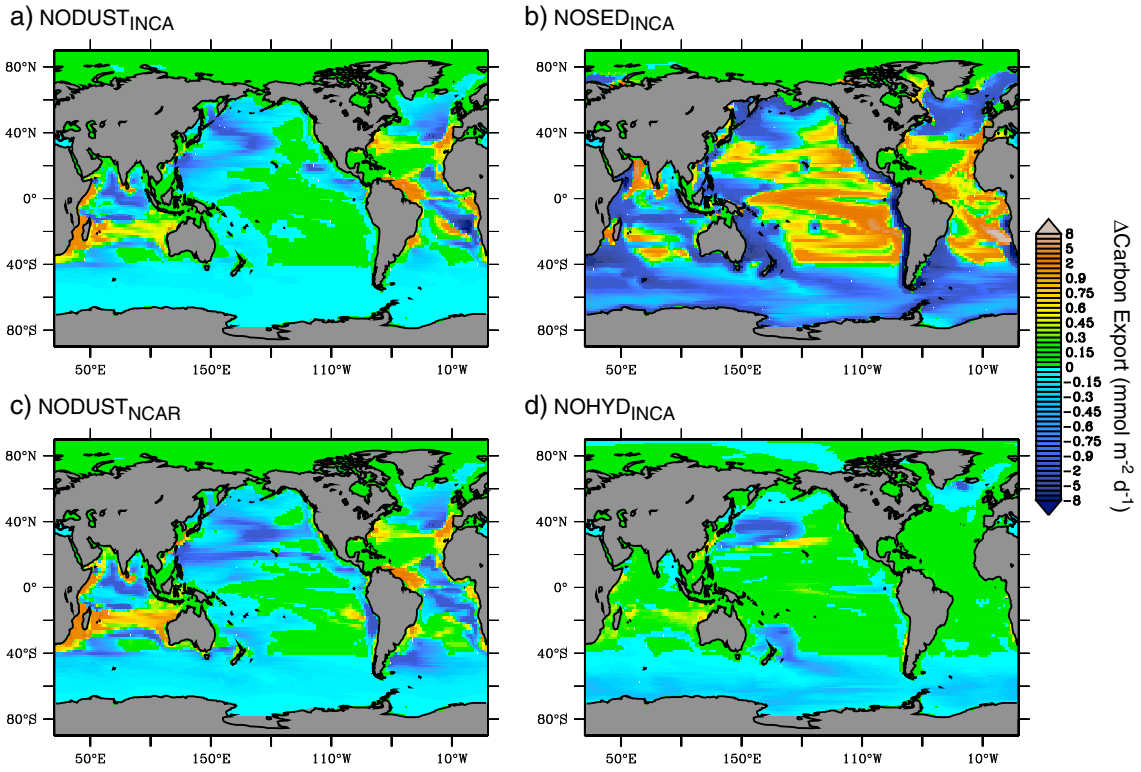

Figure 1. The change in carbon export (mmol C m^{-2} d^{-1}) for each of the experimental runs. No sedimentary (NOSED$_{NCAR}$) and No hydrothermal (NOHYD$_{NCAR}$) are virtually identical to NOSED$_{INCA}$ and NOHYD$_{INCA}$ and are not shown.

3. Results and Discussion

3.1. Carbon Cycle Impact of Different Iron Sources

CO_{2atm} is most sensitive to removal of sedimentary, then dust and finally hydrothermal inputs, with sensitivity to the assumed dust model (Table 1). For PISCES-INCA, CO_{2atm} rises by 14.5, 1.8, and 1.1 ppm when sediment, dust, and hydrothermal Fe sources are removed. When PISCES-NCAR is used, CO_{2atm} rises by 13.5, 2.3, and 1.0 ppm upon removal of sediment, dust, and hydrothermal Fe sources. The change in export production is closely tied to the CO_{2atm} changes (Table 1) by ~28 ppm CO_{2atm} increase per Pg C reduction in export ($R^2 = 0.988$, $n = 14$). Removing both sediment and hydrothermal sources in PISCES-INCA raises CO_{2atm} by 14.5 ppm (Table 1), slightly less than the sum of each effect (15.6 ppm). This arises because organic ligands introduce nonlinearity in the scaling of the iron inventory response [*Tagliabue et al.*, 2010]. In all cases, changes in CO_{2atm} and export scale well with the modifications to preformed PO_4 (Table 1).

Well-documented "downstream effects" of Fe-mediated changes in macronutrient consumption [e.g., *Sarmiento et al.*, 2004; *Tagliabue et al.*, 2008] cause a complex spatial response (Figure 1). For example, reduced export production in the Southern Ocean due to eliminated sediment Fe causes an increased supply of macronutrients to low latitudes that fuels export production in these non-Fe-limited waters (Figure 1). Accordingly, the final perturbation to export production is around two thirds of the immediate response that occurs over the first few years. The largest changes in export production are seen in the tropical Atlantic/North Pacific, offshore Southern Ocean/North Atlantic, and around Iceland/New Zealand/Japan/Southern Ocean in response to removing dust, sediment, and hydrothermal iron, respectively. Export anomalies in the Southern Ocean from dust are larger using PISCES-NCAR, in line with the greater approximately fourfold greater dust supply (Figure 1).

3.2. How Do Different Iron Sources Impact Nutrient Biogeochemistry?

In all cases, greater Fe limitation unsurprisingly led to increases in the amount of residual NO_3, PO_4, and $Si(OH)_4$ that can fuel additional production in adjacent but not Fe-limited regions. Interestingly however,

©2014. American Geophysical Union. All Rights Reserved.

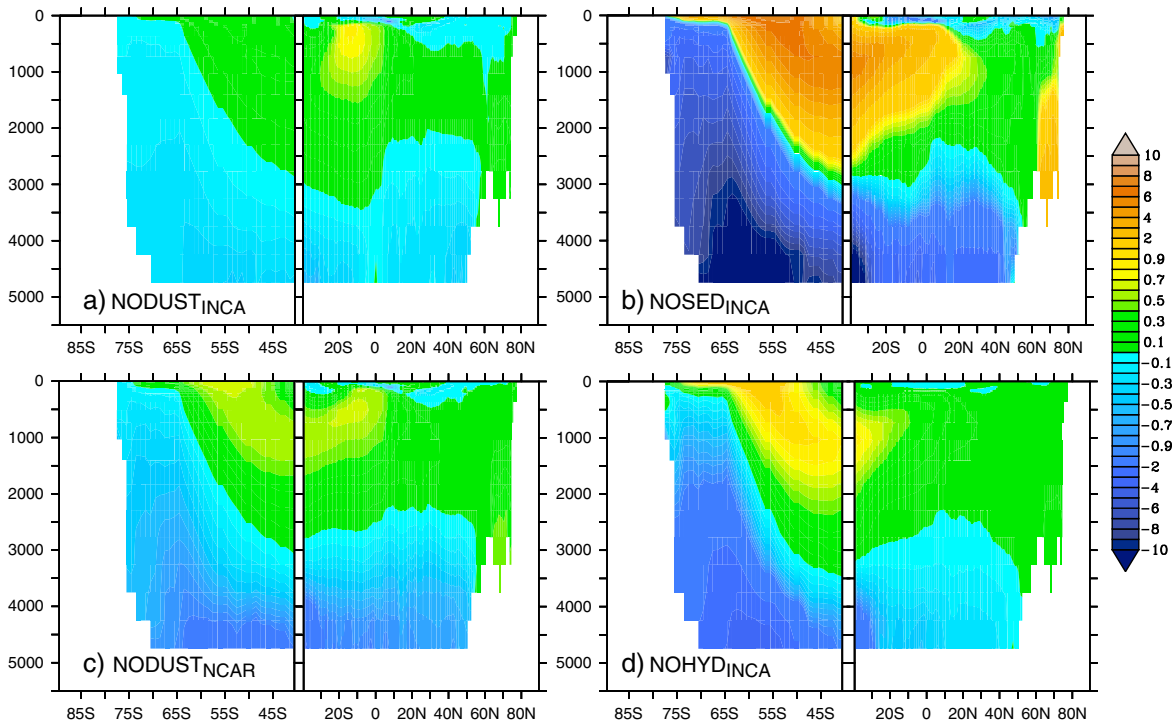

Figure 2. The zonal mean change in Si* ($Si(OH)_4$-NO_3) (mmol m^{-3}) for each of the experimental runs. Between 90°N and 40°S results are zonally averaged in the Atlantic Basin, while south of 40°S the zonal average is circumpolar. $NOSED_{NCAR}$ and $NOHYD_{NCAR}$ are virtually identical to $NOSED_{INCA}$ and $NOHYD_{INCA}$ and are not shown.

proportionally more $Si(OH)_4$ is transported than NO_3, as shown by the Si* tracer ($Si(OH)_4$-NO_3) [*Sarmiento et al.*, 2004, Figure 2]. Greater Fe limitation (e.g., due to lesser Fe input) is thought to reduce Si* from greater silicification [e.g., *Hutchins and Bruland*, 1998; *Sarmiento et al.*, 2004], but ostensibly, this should enhance $Si(OH)_4$ consumption in our simulations and reduce Si*, which is opposite to our results (Figure 2). In our simulations, the relative silicification of diatoms increases due to greater Fe limitation, but their relative abundance declines, which causes less net $Si(OH)_4$ consumption, relative to NO_3, overall. Thus, in terms of Si*, we find the impact of changing Fe limitation on the composition of the phytoplankton assemblage outweighs the physiological impact. The Si* of waters exported northward is consistently greater in response to reduced Fe inputs, and the largest effects are seen in response to the largest perturbation in Southern Ocean Fe inputs (Figure 2).

Away from localized sources, the integrated DFe column inventory ($\int$Fe, Figure S1 in the supporting information) is most sensitive to sediment and hydrothermal inputs rather than dust (across both dust models). We examined the influence of each source, by calculating the $\Delta\int$Fe for each of the simulations. When sediment sources are removed, $\Delta\int$Fe is ≤ -250 μmol Fe m^{-2} almost everywhere, reaching as low as ≤ -500 μmol Fe m^{-2} near the Southern Ocean shelves. The anomalies in $\int$Fe due to removing hydrothermal Fe are restricted to ocean ridges in the Northern Hemisphere but become much more widespread in the Southern Hemisphere (up to ≤ -500 μmol Fe m^{-2} in the Pacific Sector of the Southern Ocean). In contrast, it is only in the tropical Atlantic and northwest Indian Ocean where dust anomalies are significant (for either dust model).

3.3. The Most Significant Iron Source?

The relative role of different Fe sources in controlling certain properties of the system depends firstly on the property of interest and secondly on the assumptions regarding dust deposition. If we are concerned with $\int$Fe, then sediment sources are most important for ~74% of the ocean area, followed by hydrothermal sources for ~23%, and dust for just ~2% (regardless of the dust model employed, Table 2). Hydrothermalism is most important in the eastern Pacific and the Pacific and Indian sectors of the Southern Ocean, with dust restricted to the tropical Atlantic and sediment sources dominating elsewhere (Figure 3). However, if we then turn our attention to carbon export, the picture changes slightly and despite sediment sources remaining dominant at 79–81% of the ocean area, dust is now more important at 12–16% and hydrothermalism is less important at

©2014. American Geophysical Union. All Rights Reserved.

Table 2. A Summary of the Relative Role Played by Different Iron Sources in Governing the Column Inventory of Fe (∫Fe) and Carbon Export at 100 m (in Percent of Ocean Surface Area) Across the Range of Experiments[a]

Dominant Iron Source	Dust Source	Driver of Anomalies (% Ocean Area)	
		∫Fe	Carbon Export
Dust	INCA	2.0	12.4
Sediment	INCA	74.4	81.3
Hydrothermal	INCA	23.6	3.2
Multiple	INCA	0	3.1
Dust	NCAR	2.6	15.9
Sediment	NCAR	74.3	78.8
Hydrothermal	NCAR	23.1	2.2
Multiple	NCAR	0	3.1

[a]In some regions, multiple sources of iron are equally significant.

~3%. (Table 2 and Figure 3, depending on the dust model used). Hydrothermal control of export production is restricted to areas adjacent to shallow sources (near Iceland and Japan) or localized upwelling, with the influence of dust apparent in parts of the Pacific and Indian Oceans. In 3% of the ocean area (always on the shelf) more than one Fe source exerts equal control.

The relative impact of a given source on CO_{2atm} is regulated by its control on export production. This is not surprising given the extent to which CO_{2atm} anomalies are driven by changes in global carbon export (section 3.1). Less clear is the relationship between the extent to which a given source regulates ∫Fe and CO_{2atm}. A good example in this context is hydrothermal input, which controls ∫Fe over almost 25% of the ocean (Table 2) but contributes little to CO_{2atm} (Table 1). Conversely, dust input regulates ∫Fe over only ~2% of the ocean but contributes slightly more to CO_{2atm}. These results highlight the role of ocean ventilation and organic ligands (see section 3.4) in regulating

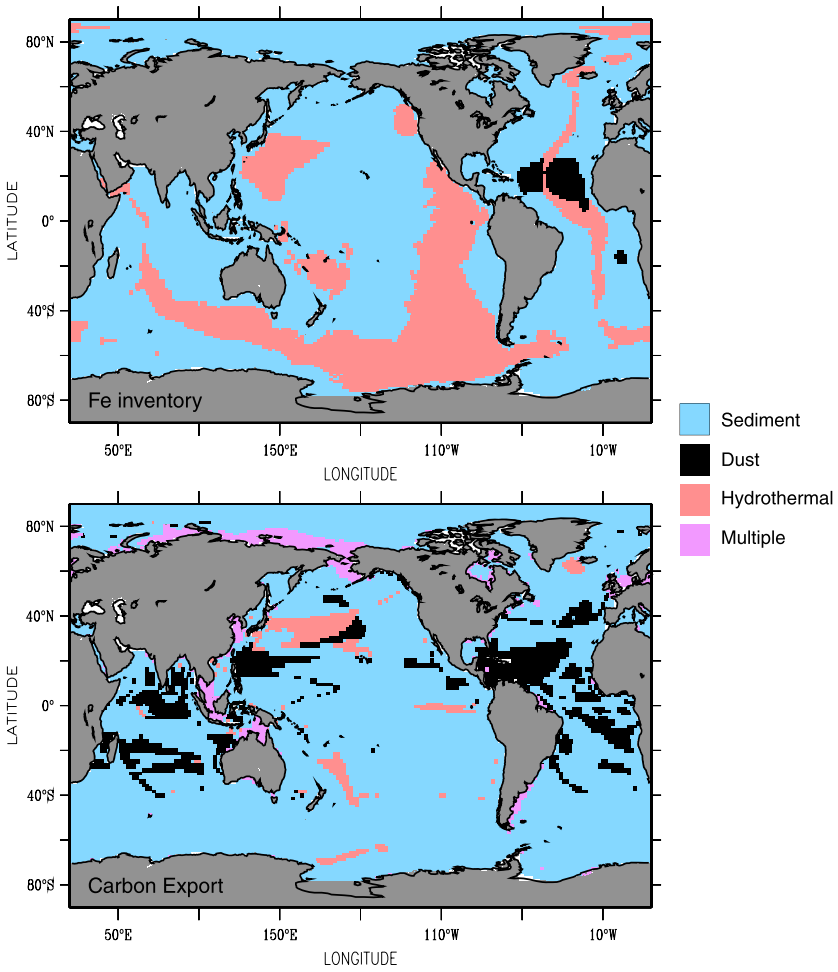

Figure 3. The source of Fe that dominates the anomalies in the column integrated (top) Fe inventory and (bottom) carbon export.

©2014. American Geophysical Union. All Rights Reserved.

the sensitivity of export production to subsurface Fe sources. Hydrothermal input is clearly a major control on the interior distributions of dissolved Fe but relies on deepwater ventilation for this Fe to be transported to the surface dwelling biota [*Tagliabue et al*., 2010]. Far from sources, organic ligands might act to stabilize the Fe inventory and thus buffer the impact of Fe input variability. In contrast, dust supply of Fe arrives directly at the surface and does not require physical processes to modulate its transfer to the biota.

3.4. Uncertainties in Iron Cycling

Varying our assumptions regarding the concentrations of DFe-binding ligands has significant impacts on CO_{2atm}. For example, simply halving or doubling the ligand concentration (from 0.3 to 1.2 nM) modifies CO_{2atm} by −5.1 or +5.4 ppm (Table 1), which is greater than the dust or hydrothermal effects. Taken in combination with changing Fe inputs, modifying ligand concentrations can either accentuate or dampen the previously seen impact. For example, halving or doubling ligand concentrations alongside removing sedimentary Fe input modifies CO_{2atm} by +10.0 or +18.2 ppm, respectively, compared to +14.5 ppm when ligand concentrations were not modified (Table 1). Overall, the effects of parallel ligand variations introduce additional changes on the order of 10–25%. The ligand scenarios we have examined remain well within the concentrations observed (e.g., 0.1 to $>$ 2nM) [*Gledhill and Buck*, 2012], thereby highlighting the importance of organic complexation to the Fe inventory and CO_{2atm}.

4. Future Considerations

4.1. Modifications to Atmospheric CO_2

Reduced dust deposition of iron seen as a driver of the rise in CO_{2atm} from glacial to interglacial epochs [*Lourantou et al*., 2010; *Martinez-Garcia et al*., 2011; *Ziegler et al*., 2013]. This is at odds with our findings that the CO_{2atm} sensitivity to dust iron to be of the order of ~ 2 ppm (Table 1). This arises because, while dust input was the dominant Fe source in our simulations (Table 1), it is not the major regulator of export production in the Southern Ocean, which plays the dominant role in regulating CO_{2atm}. Focus on constraining the glacial Fe supply to the Southern Ocean is thus important in this regard. Moreover, changes to ligand concentrations can have a larger impact than dust and substantial uncertainties exist in constraining their cycling [*Gledhill and Buck*, 2012].

The concept that relative $Si(OH)_4$ export from the Southern Ocean to low latitudes is positively related to Southern Ocean Fe supply due to varying silicification [*Matsumoto et al*., 2002] is not supported (Figure 2). We find that the relative amount of diatoms, rather than their degree of silicification, is dominant in regulating the relative export of $Si(OH)_4$. Diatoms become less competitive as the Fe input is decreased and relatively greater $Si(OH)_4$ is exported with reduced iron input to the Southern Ocean (Figure 2). Thus silicic acid leakage may work against the general CO_{2atm} tendency rather than being a driver of it.

4.2. Characterizing Iron Sources

A number of simplifying assumptions in our representations of the Fe inputs to the ocean could be improved in the future to yield more robust determinations of their relative role in regulating CO_{2atm} and ∫Fe. For example, accounting for dust mineralogy and associated variability in Fe content/solubility should be addressed, although this will conceivably have a greater impact on local biogeochemistry and ∫Fe than on CO_{2atm}. In addition, recent work has highlighted variability in sediment [*Homoky et al*., 2013] and hydrothermal [*Saito et al*., 2013] inputs that would be important to constrain in future models. Our prior understanding, and its inclusion in our model, was that shelf depth, and in particular, the degree of carbon oxidation was the main driver of Fe efflux [*Elrod et al*., 2004]. However, *Homoky et al*. [2013] have noted that some shelves can be less important sources of Fe than their depth and oxygen content would indicate. In a similar fashion, we assume that the hydrothermal Fe flux is regulated by ridge spreading rate, as parameterized by a constant DFe/Helium ratio [*Tagliabue et al*., 2010]. Yet recent observations [*Saito et al*., 2013] suggest that there might be less variability in Fe input from hydrothermal vents than there is for helium. To respond to this, we have upscaled the DFe/Helium ratio in this study, but the connection to ridge spreading rate remains. All sources clearly also do not only supply DFe, and although our model simulates particulate Fe, we do not consider unique sources of particulate Fe. More observational and specific modeling work is therefore needed to better understand how shelf depth and other factors interact to regulate sedimentary Fe input and how

©2014. American Geophysical Union. All Rights Reserved.

the local conditions of different hydrothermal systems regulate the dissolved Fe input distinctly to that of Helium. The ongoing expansion of Fe observations as part of the GEOTRACES project will prove invaluable in this regard.

5. Conclusions

We have quantified the CO_{2atm} sensitivity to Fe supply from dust, sediments, and hydrothermal vents using two different representations of dust supply that differ by a factor of ~4 in their Southern Ocean deposition. We find CO_{2atm} to be most sensitive to sediment iron supply, with a relatively weak sensitivity to either representation of dust deposition or hydrothermal input. This arises due to the overwhelming role for sediment supply in regulating Southern Ocean export production. While hydrothermal input is crucial in governing the Fe inventory for ~25% of the ocean, its impact on export production and CO_{2atm} is regulated by ocean ventilation. Changing Fe supply to the ocean modifies the relative export of $Si(OH)_4$ to low latitudes, but we find that $Si(OH)_4$ export rises when Fe supply is reduced due to lesser diatom productivity, contrary to the silicic acid leakage hypothesis [*Matsumoto et al.*, 2002]. Interestingly, we find that modifying assumptions regarding the concentration of ligands has a potentially very large effect on CO_{2atm}, particularly in combination with Fe source changes.

Acknowledgments

This work made use of the facilities of N8 HPC provided and funded by the N8 consortium and EPSRC (grant EP/K000225/1). The Centre is coordinated by the Universities of Leeds and Manchester. We thank Yves Balkanski and Natalie Mahowald for sharing the dust deposition estimates from the INCA and NCAR models, respectively, and two anonymous reviewers for their comments that improved the final manuscript.

The Editor thanks two anonymous reviewers for their assistance in evaluating this paper.

References

Aumont, O., and L. Bopp (2006), Globalizing results from ocean in situ iron fertilization studies, *Global Biogeochem. Cycles*, *20*, GB2017, doi:10.1029/2005GB002591.

Boyd, P. W., and M. J. Ellwood (2010), The biogeochemical cycle of iron in the ocean, *Nat. Geosci.*, *3*(10), 675–682, doi:10.1038/ngeo964.

Elrod, V. A., W. M. Berelson, K. H. Coale and K. S. Johnson (2004), The flux of iron from continental shelf sediments: A missing source for global budgets, *Geophys. Res. Lett.*, *31*, 675–682, doi:10.1029/2004gl020216.

Gledhill, M., and K. N. Buck (2012), The organic complexation of iron in the marine environment: A review, *Frontiers in Microbiology*, *3*(69), 675–682, doi:10.3389/fmicb.2012.00069.

Homoky, W., S. G. John, T. M. Conway, and R. A. Mills (2013), Distinct iron isotopic signatures and supply from marine sediment dissolution, *Nat. Commun.*, *4*, 2143, doi:10.1038/ncomms3143.

Huneeus, N., et al. (2011), Global dust model intercomparison in AeroCom phase I, *Atmos. Chem. Phys.*, *11*, 7781–7816, doi:10.5194/acp-11-7781-2011.

Hutchins, D. A., and K. W. Bruland (1998), Iron-limited diatom growth and Si:N uptake ratios in a coastal upwelling regime, *Nature*, *393*, 561–564, doi:10.1038/31203.

Lancelot, C., A. de Montety, H. Goosse, S. Becquevort, V. Schoemann, B. Pasquer, and M. Vancoppenolle (2009), Spatial distribution of the iron supply to phytoplankton in the Southern Ocean: A model study, *Biogeosciences*, *6*(12), 2861–2878, doi:10.5194/bg-6-2861-2009.

Kohfeld, K. E., and A. Ridgwell (2009), Glacial-interglacial variability in atmospheric CO_2, in *Surface Ocean-Lower Atmosphere Processes*, edited by C. L. Quéré and E. S. Saltzman, AGU, Washington, D. C., doi:10.1029/2008GM000845.

Lourantou, A., J. V. Lavrič, P. Köhler, J.-M. Barnola, D. Paillard, E. Michel, D. Raynaud, and J. Chappellaz (2010), Constraint of the CO_2 rise by new atmospheric carbon isotopic measurements during the last deglaciation, *Global Biogeochem. Cycles*, *24*, GB2015, doi:10.1029/2009GB003545.

Mahowald, N., A. Baker, G. Bergametti, N. Brooks, R. Duce, T. Jickells, N. Kubilay, J. Prospero, and I. Tegen (2005), Atmospheric global dust cycle and iron inputs to the ocean, *Global Biogeochem. Cycles*, GB4025, doi:10.1029/2004GB002402.

Martin, J. H. (1990), Glacial-interglacial CO_2 change: The iron hypothesis, *Paleoceanography*, *5*(1), 1–13, doi:10.1029/Pa005i001p00001.

Martinez-Garcia, A., A. Rosell-Melé, S. L. Jaccard, W. Geibert, D. M. Sigman, and G. H. Haug (2011), Southern Ocean dust-climate coupling over the past four million years, *Nature*, *476*, 312–315.

Matsumoto, K., J. L. Sarmiento, and M. A. Brzezinski (2002), Silicic acid leakage from the Southern Ocean: A possible explanation for glacial atmospheric pCO_2, *Global Biogeochem. Cycles*, *16*(3), 1031, doi:10.1029/2001GB001442.

Middelburg, J. J., K. Soetaert, and P. M. J. Herman (1997), Empirical relationships for use in global diagenetic models, *Deep Sea Res., Part I*, *44*(2), 327–344.

Moore, J. K., and O. Braucher (2008), Sedimentary and mineral dust sources of dissolved iron to the world ocean, *Biogeosciences*, *5*(3), 631–656, doi:10.5194/bg-5-631-2008.

Saito, M., A. E. Noble, A. Tagliabue, T. J. Goepfert, C. H. Lamborg, and W. J. Jenkins (2013), Slow-spreading submarine ridges in the South Atlantic as a significant oceanic iron source, *Nat. Geosci.*, *6*, 775–779, doi:10.1038/ngeo1893.

Sarmiento, J. L., and J. C. Orr (1991), 3-Dimensional simulations of the impact of Southern-Ocean nutrient depletion on atmospheric CO_2 and ocean chemistry, *Limnol. Oceanogr.*, *36*(8), 1928–1950.

Sarmiento, J. L., N. Gruber, M. A. Brzezinski, and J. P. Dunne (2004), High-latitude controls of thermocline nutrients and low latitude biological productivity, *Nature*, *427*, 56–60, doi:10.1038/nature02127.

Tagliabue, A., L. Bopp, and O. Aumont (2008), Ocean biogeochemistry exhibits contrasting responses to a large scale reduction in dust deposition, *Biogeosciences*, *5*, 11–24.

Tagliabue, A., L. Bopp, and O. Aumont (2009), Evaluating the importance of atmospheric and sedimentary iron sources to Southern Ocean biogeochemistry, *Geophys. Res. Lett.*, *36*, L13601, doi:10.1029/2009GL038914.

Tagliabue, A., et al. (2010), Hydrothermal contribution to oceanic dissolved iron inventory, *Nat. Geosci.*, *3*, 252–256, doi:10.1038/ngeo818.

Tagliabue, A., T. Mtshali, O. Aumont, A. R. Bowie, M. B. Klunder, A. N. Roychoudhury, and S. Swart (2012), A global compilation of dissolved iron measurements: Focus on distributions and processes in the Southern Ocean, *Biogeosciences*, *9*, 2333–2349, doi:10.5194/bg-9-2333-2012.

Wagener, T., C. Guieu, R. Losno, S. Bonnet, N. Mahowald (2008), Revisiting atmospheric dust export to the Southern Hemisphere Ocean: Biogeochemical implications, *Global Biogeochem. Cycles*, *22*, GB2006, doi:10.1029/2007GB002984.

Ziegler, M., P. Diz, I. R. Hall, and R. Zahn (2013), Millennial-scale changes in atmospheric CO_2 levels linked to the Southern Ocean carbon isotope gradient and dust flux, *Nat. Geosci.*, *6*, 457–461.

©2014. American Geophysical Union. All Rights Reserved.